Available online at www.sciencedirect.com
SCIENCE DIRECT
J. of Supercritical Fluids 36 (2005) 106–117
THE JOURNAL OF Supercritical Fluids
www.elsevier.com/locate/supflu

Viscosity of pure supercritical fluids

Marcelo S. Zabaloy [a,*], Victor R. Vasquez [b], Eugénia A. Macedo [c]

[a] *Planta Piloto de Ingeniería Química, Universidad Nacional del Sur CC 717, 8000 Bahía Blanca, Argentina*
[b] *Mail Stop 170, Chemical Engineering Department, University of Nevada-Reno, 1664 N. Virginia St., Reno, NV 89557-0136, USA*
[c] *LSRE-Laboratory of Separation and Reaction Engineering, Departamento de Engenharia Química, Faculdade de Engenharia da Universidade do Porto, Rua do Dr. Roberto Frias, 4200-465 Porto, Portugal*

Received 16 September 2004; accepted 17 May 2005

Abstract

In this work, we propose a model for representing the viscosity of supercritical pure fluids over a wide range of conditions. A given pure real fluid is represented as a Lennard–Jones (LJ) fluid having effective values of the LJ intermolecular potential parameters. The LJ fluid is actually a corresponding states fluid where the dimensionless variables have, as a distinguishing feature, a dependency on parameters meaningful at molecular level. We have paid special attention to the qualitative behavior of the model when used beyond the conditions of the supporting molecular LJ simulation data. The model is able to correlate the pure compound viscosity of real supercritical fluids over a wide range of conditions with average absolute-value relative deviations less than or equal to 7% in most cases. The correlation needs two adjustable parameters per pure compound.

Keywords: Viscosity; Supercritical real fluids; Model; Molecular simulation; Lennard–Jones

1. Introduction

Practical use of supercritical fluids requires reliable models for their thermophysical properties. Supercritical extraction and processing typically take place at conditions where a solute (or a number of them), and eventually a co-solvent, are highly diluted in a supercritical solvent. For this reason, models used to represent the thermophysical properties of such diluted mixtures should match the pure solvent limit or at least approach it with an acceptable level of error, which implies, as a requirement, the availability of accurate models for pure supercritical fluids. Such models should preferably make reference to some adopted form for the intermolecular potential function. In this work, we concentrate on modeling the viscosity of pure real fluids at temperatures and pressures beyond their critical values, i.e., at supercritical conditions. The model is based on the well-known Lennard–Jones intermolecular potential.

Viscosity is a complex property to model because density strongly influences its temperature dependence. At high density, viscosity decreases with temperature, while the behavior is the opposite at low density. At intermediate density values, local extrema appear for viscosity as a function of temperature. This involved behavior implies crossing viscosity versus pressure isotherms.

There are different kinds of models for viscosity available in the literature. Some of them do not specify an intermolecular potential function (see, e.g., Ref. [1]) and hence they are regarded as purely empirical correlations [2]. On the other hand, models that do specify an intermolecular potential function are often limited to subcritical fluids and/or require the use of compound-specific correlations for the pressure–density–temperature relationship (see, e.g., Ref. [3]).

Zabaloy et al. [4] discussed the different ways in which molecular simulation data can be used. In this work, we

* Corresponding author. Tel.: +54 291 486 1700x232; fax: +54 291 486 1600.
E-mail addresses: mzabaloy@plapiqui.edu.ar (M.S. Zabaloy), vvasquez@engr.unr.edu (V.R. Vasquez), eamacedo@fe.up.pt (E.A. Macedo).

0896-8446/$ – see front matter © 2005 Elsevier B.V. All rights reserved.
doi:10.1016/j.supflu.2005.05.002

Nomenclature

AAD%	average absolute-value percent relative deviation $= (100/\mathrm{NP})\sum_{i=1}^{\mathrm{NP}}\lvert\eta_{\mathrm{calc}} - \eta_{\mathrm{exp}}\rvert/\eta_{\mathrm{exp}}$
cp	critical point
CS	corresponding states
EOS	equation of state
k	Boltzmann constant
liq	saturated liquid
LJ	Lennard–Jones
m	mass of one molecule
Max AD%	maximum absolute-value percent relative $= \max_{i=1}^{\mathrm{NP}}\{100\lvert\eta_{\mathrm{calc}} - \eta_{\mathrm{exp}}\rvert/\eta_{\mathrm{exp}}\}$
MD	molecular dynamics
N	number of molecules
N_{A}	Avogadro's number
NP	number of data points
P	absolute pressure
P_{c}	critical pressure
P_{r}	practical reduced pressure
P^{+}_{SFE}	LJ melting P^{+}
PVT	pressure–volume–temperature
r	intermolecular distance
RP	Rowley and Painter
S_{σ}	slope for σ as a function of T_{r}
SFE	solid–fluid equilibrium
T	absolute temperature
T_{c}	critical temperature
T_{r}	practical reduced temperature
TP	triple point
U	intermolecular potential energy
V	system volume
vap	saturated vapor
VLE	vapor–liquid equilibrium
VTD	viscosity–temperature–density
z	compressibility factor

Greek letters

ε	depth of the LJ potential well
η	(Newtonian shear) viscosity
η_0	viscosity at zero density
η_{exp}	experimental viscosity
η_{calc}	calculated viscosity
$\rho^{+}_{\mathrm{fluid,SFE}}$	dimensionless density of dense LJ fluid in equilibrium with LJ solid
ρ	mole density (e.g., mol l^{-1} units)
ρ_{c}	critical mole density (e.g., mol l^{-1} units)
σ	LJ separation distance at zero energy
σ_{c}	critical value of σ

propose a model for the viscosity of pure supercritical fluids, which makes use of molecular simulation results for the Lennard–Jones (LJ) fluid. The link between the dimensionless pressure, temperature, density and viscosity is set by analytical functions designed so that recent LJ molecular simulation results are reproduced over a wide range of conditions. The use we make in this work of a pressure–density–temperature LJ equation of state (EOS), on top of providing a more consistent LJ reference, makes possible to avoid the use of compound-specific PVT EOSs for computing densities from the set pressure and temperature.

A key problem we deal with here is the need of setting up proper interpolation and extrapolation schemes. Zabaloy et al. [4] raised this issue and proposed criteria to guide the definition of such schemes, but left the extrapolation problem unsolved. The problem of extrapolating arises when it is required to calculate the viscosity of a real fluid at temperature and density conditions which correspond to LJ dimensionless temperature and density coordinates beyond the range of the supporting molecular simulation data. On the other hand, interpolation between states where the LJ fluid exists as an homogeneous (one-phase) stable fluid is required when a real homogeneous fluid is at temperature and density conditions corresponding to LJ dimensionless coordinates where the LJ fluid is actually heterogeneous (e.g., when the LJ fluid is in a state of vapor–liquid equilibrium). According to our experience, the problem of interpolating–extrapolating molecular simulation data is by no means trivial. In this work, we propose a solution to this problem.

The basic methodology in this work is the same than that of Ref. [4]. One of the fundamental differences between this work and Ref. [4] is the introduction of extrapolation schemes. On the other hand, adjustable parameters were not used in Ref. [4] due to the exploratory nature of such work. In contrast, in the present application-oriented work, we introduce a couple of suitable adjustable parameters to improve the model performance.

2. The Lennard–Jones fluid

The expression for the Lennard–Jones intermolecular potential is as follows:

$$u(r) = 4\varepsilon\left[\left(\frac{\sigma}{r}\right)^{12} - \left(\frac{\sigma}{r}\right)^{6}\right] \tag{1}$$

where r is the intermolecular distance, u the intermolecular potential energy, ε the depth of the LJ potential well and σ is the LJ separation distance at zero energy. The LJ fluid is simple but realistic: it qualitatively reproduces the viscous behavior observed for real fluids over a wide range of conditions [4].

The values of the physical properties of the LJ fluid are accessed through computer experiments. This is also the case for every model fluid, which, as the LJ fluid, only exists within a mathematical universe. The phase diagram of the LJ fluid is known [4]. In spite of the relative simplicity of Eq. (1), vapor–liquid, solid–vapor and solid–fluid transitions appear in the LJ phase diagram [4]. From this, it is clear that Eq. (1) captures the essential behavior found for real substances.

The LJ reduced temperature T^+, reduced pressure P^+, reduced density ρ^+ and reduced viscosity η^+ are conventionally defined as follows:

$$T^+ = \frac{kT}{\varepsilon} \tag{2}$$

$$P^+ = \frac{P\sigma^3}{\varepsilon} \tag{3}$$

$$\rho^+ = \frac{N}{V}\sigma^3 = N_A\rho\sigma^3 \tag{4}$$

$$\eta^+ = \eta\frac{\sigma^2}{\sqrt{m\varepsilon}} \tag{5}$$

where k is the Boltzmann constant, T the absolute temperature, P the absolute pressure, N the number of molecules, V the system volume, N_A Avogadro's number, ρ the mole density in units such as moles per liter, η the Newtonian shear viscosity and m is the mass of one molecule.

3. Lennard–Jones viscosity

Rowley and Painter (RP) [5] computed LJ shear viscosities at conditions covering wide ranges of density and temperature ($0.8 \le T^+ \le 4$), using the method of molecular dynamics (MD). They built an analytical equation by correlating their MD results. Such analytical equation relates the viscosity η^+ to T^+ and ρ^+, and it requires calculating the LJ reduced viscosity limit at zero density η_0^+ which Rowley and Painter correlated as a function of T^+ (see Ref. [5] for details).

Zabaloy et al. [4] slightly changed the form of the RP Lennard–Jones analytical η^+ versus (T^+, ρ^+) function and re-fitted its parameters so that certain qualitative behavior constraints, considered appropriate for a model to be used in wide ranges of temperature and density, would be met by their LJ analytical viscosity–temperature–density (VTD) relationship. Zabaloy et al. [4] changed the RP analytical function in anticipation of setting up robust extrapolation schemes for cases where the real fluid conditions fall outside the original ranges of applicability of the LJ VTD analytical relationship. Although Zabaloy et al. [4] identified the need for extrapolation schemes as a relevant issue, within the context of molecular-simulation-based engineering-oriented real-fluid model building, they left the problem of defining such schemes as an open question.

Extrapolation recipes may consist of truncated Taylor expansions of the function to be extrapolated. Such approach generally implies discontinuities in higher order derivatives at the boundary where the switch between the original function and the extrapolating function takes place.

In this work, we have found a way to avoid discontinuity-carrying extrapolation recipes for the LJ viscosity–temperature–density relationship. We did so by choosing a functional form and sign restrictions on parameter values consistent with both, the RP supporting LJ molecular simulation data and the VTD qualitative behavior constraints that Zabaloy et al. [4] identified. Such constraints are met by the functional form + parameter values here reported, within and beyond the range of the supporting RP LJ molecular simulation data, as shown below.

Zabaloy et al. [4] used the same expression for the LJ viscosity limit at zero density (η_0^+) than Rowley and Painter [5]. Such expression cannot be used for $T^+ > 4$, i.e., beyond the range of applicability given in Ref. [5], because the trend for η_0^+ versus T^+ becomes opposite to the correct one for $T^+ > 4$.

4. New Lennard–Jones analytical viscosity representation

In this work, we use the following analytical form for the LJ viscosity–temperature–density relationship.

$$\eta^+ = \eta_0^+ + \sum_{i=2}^{10}\sum_{j=1}^{3} b_{ji}\frac{(\rho^+)^i}{(T^+)^{j-1}} \tag{6}$$

where η_0^+ does not correspond to Ref. [5]. We rather use for η_0^+ the Chapman–Enskog equation coupled to the Neufeld–Janzen–Aziz expression for the collision integral, as presented in Eqs. (9-3.9) and (9-4.3) of Ref. [6], which are applicable within the wide range $0.3 \le T^+ \le 100$. In this work, we rewrite Eqs. (9-3.9) of Ref. [6], in terms of the above defined dimensionless variables, as follows:

$$\eta_0^+ = \frac{0.176288(T^+)^{1/2}}{\Omega_\upsilon(T^+)} \tag{7}$$

where $\Omega_\upsilon(T^+)$ is the collision integral, which is a function of T^+, as its single independent variable, and is given in Eqs. (9-4.3) of Ref. [6].

The form of Eq. (6) is different from the (exponential) form of Eq. (15) in Ref. [4]. As it will become clear below, such difference in form is of much more fundamental importance than it may seem at first sight.

4.1. Viscosity constraints

Based on both, LJ molecular simulation viscosity data and real fluid viscosity data, Zabaloy et al. [4] concluded that the following constraints on the derivatives of the LJ viscosity were suitable for an analytical model to be used over a wide range of conditions:

$$\left(\frac{\partial\eta^+}{\partial\rho^+}\right)_{\rho^+=0} = 0 \tag{8}$$

$$\frac{\partial\eta^+}{\partial\rho^+} > 0, \quad \text{for } \rho^+ > 0 \tag{9}$$

$$\frac{\partial(\partial\eta^+/\partial\rho^+)}{\partial\rho^+} > 0, \quad \text{for } \rho^+ \ge 0 \tag{10}$$

$$\frac{\partial(\partial\eta^+/\partial\rho^+)}{\partial T^+} < 0, \quad \text{for } \rho^+ > 0 \tag{11}$$

Eq. (8) corresponds to a flat viscosity η^+ versus density ρ^+ curve at constant temperature T^+ when ρ^+ approaches zero. Constraint (9) implies a monotonic increase for viscosity with density at constant temperature. Restriction (10) sets a monotonic increase of the viscosity versus density slope with density at constant temperature. Constraint (11) establishes that, at constant density, the viscosity versus density slope decreases with temperature. As Zabaloy et al. [4] discussed, constraints (8)–(11) set a qualitative viscous behavior simpler than the observed one, both, for the Lennard–Jones fluid and for real fluids. However, they grasp the essential known viscous behavior of fluids, over a wide range of conditions, thus providing a convenient reference viscosity description with well-defined qualitative trends (see Ref. [4] for more details).

Zabaloy et al. [4] imposed restriction (8) by construction within the analytical η^+ versus (T^+, ρ^+) function that they proposed, and restrictions (9)–(11) during the parameter fitting process. They verified the fulfillment of restrictions (9)–(11) for more than 12,000 regularly spaced points in the domain $0.8 \le T^+ \le 4$ and $0 \le \rho^+ \le 1$. Yet, their parameters values [4] do not guarantee meeting the constraints (9)–(11) outside the tested range.

On the other hand, Eq. (6) implies the following expressions for the partial derivatives involved in the above presented constraints:

$$\frac{\partial\eta^+}{\partial\rho^+} = \sum_{i=2}^{10}\sum_{j=1}^{3} i b_{ji} \frac{(\rho^+)^{i-1}}{(T^+)^{j-1}} \tag{12}$$

$$\frac{\partial(\partial\eta^+/\partial\rho^+)}{\partial\rho^+} = \sum_{i=2}^{10}\sum_{j=1}^{3} i(i-1) b_{ji} \frac{(\rho^+)^{i-2}}{(T^+)^{j-1}} \tag{13}$$

$$\frac{\partial(\partial\eta^+/\partial\rho^+)}{\partial T^+} = \sum_{i=2}^{10}\sum_{j=1}^{3} i(1-j) b_{ji} \frac{(\rho^+)^{i-1}}{(T^+)^{j}} \tag{14}$$

Notice that, since η_0^+ depends only on T^+, the derivative of η_0^+ with respect to ρ^+ is zero. Eq. (12) reflects this fact.

It can be shown that Eq. (12) meets restriction (8). Observe that all terms in Eq. (12) are proportional to some integer non-zero power of density and hence they all vanish as density tends to zero. A key point in this work is that Eqs. (12)–(14), respectively, meet restrictions (9)–(11) if we force all b_{ji} parameters to be positive. Notice that the factors i [Eq. (12)] and the factors $i(i-1)$ [Eq. (13)] are all positive for the i range of variation within Eqs. (12) and (13). On the other hand, the factors $i(1-j)$ are zero or negative for the i and j ranges of variation within Eq. (14). The key feature of Eq. (6) coupled to the following restrictions:

$$b_{ji} > 0, \quad \text{for all } (i, j) \text{ pairs} \tag{15}$$

is that constraints (8)–(11) will be met not only within the T^+ and ρ^+ ranges of the RP molecular simulation data we used here to compute the values of the b_{ij} parameters but also at any arbitrary (positive) values of T^+ and ρ^+ as long as the wide T^+ range of Eq. (7) is not exceeded. Therefore, the simple extrapolation recipe in this work, to be applied when the ρ^+ (or the T^+) value exceeds the range of the RP LJ molecular simulation viscosity data, consists of simply using the very same equation resulting from the imposed reproduction of RP data, i.e., Eq. (6) [with the (positive) b_{ij} parameters we report later in this article], coupled to Eq. (7).

Using Eq. (6) for computing the viscosity η^+, with $b_{ji} > 0$, at any values of T^+ and ρ^+, implies that the viscosity and all its partial derivatives (of any degree) with respect to T^+ and ρ^+ are in this model continuous functions of T^+ and ρ^+.

4.2. General Lennard–Jones viscosity parameters

We fitted the b_{ij} parameters of Eq. (6) so as to reproduce the 134 Rowley and Painter [5] LJ viscosity data left after excluding 37 data points with T^+ and ρ^+ values at which the LJ fluid is unstable, i.e., not homogeneous. The 37 data points we screened out correspond, at infinite time, to conditions of vapor–liquid equilibrium for the LJ fluid. The 134 RP molecular simulation LJ viscosity data we used here have an average uncertainty of 10.3% and a maximum uncertainty of 24.6% [5]. We report the values for the b_{ij} parameters that we computed in this work in Table 1. Notice that all of them are positive. These values correspond to a bias of 0.005% and to an average absolute-value percent relative deviation (AAD%) of 4.6% with respect to the 134 RP data points we accepted, being the maximum absolute-value percent relative deviation equal to 13.9%. Hence, Eq. (6) (Table 1) reproduces the RP original molecular simulation 134-point-data-set within its reported uncertainty. These AAD% and bias values imply that the RP LJ molecular simulation data support the use of constraints (8)–(11) and/or the use of Eq. (6) coupled to restrictions (15).

The parameters of Table 1, which are general for the LJ fluid, make possible to connect molecular level parameters to macroscopic properties through fast calculations performed using Eq. (6). Due to the use of Eq. (7) and to the fulfillment of restrictions (8)–(11) by Eq. (6) coupled to the parameters given in Table 1, the viscosity–temperature–density analytical representation we use in this work for the LJ fluid should not be regarded as the result of a blind polynomial fit. A proper qualitative behavior is given by Eq. (6) (Table 1) at any temperature–density condition: within and beyond the range of the supporting molecular simulation data. Fig. 1 shows a set of viscosity versus density isotherms generated using Eq. (6) (Table 1). The temperature values $T^+ = 0.8$ (subcritical) and $T^+ = 4$ (supercritical) correspond to the limits of the temperature range of the original RP LJ data. As expected, these two isotherms are consistent with restrictions (8)–(11). It can be seen that η^+ at $T^+ = 0.8$ increases faster with

Table 1
Values for the dimensionless parameters of Eq. (6) obtained in this work

j	i	b_{ji}	j	i	b_{ji}	j	i	b_{ji}
1	2	1.325875×10^{0}	1	5	0.510490×10^{0}	1	8	0.110954×10^{0}
2	2	4.529702×10^{-11}	2	5	1.477943×10^{-11}	2	8	7.921571×10^{-4}
3	2	4.759355×10^{-11}	3	5	3.471516×10^{-11}	3	8	3.712390×10^{-2}
1	3	0.411250×10^{0}	1	6	0.441143×10^{0}	1	9	8.260164×10^{-2}
2	3	1.598922×10^{-2}	2	6	1.478254×10^{-12}	2	9	1.466775×10^{0}
3	3	2.341807×10^{-11}	3	6	5.342499×10^{-6}	3	9	2.822336×10^{0}
1	4	$2.053585\ 10^{-4}$	1	7	$0.253873\ 10^{0}$	1	10	2.287980×10^{-13}
2	4	1.682684×10^{-7}	2	7	4.255116×10^{-4}	2	10	7.244097×10^{-2}
3	4	1.428941×10^{-11}	3	7	1.003290×10^{-7}	3	10	0.309918×10^{0}

density than η^+ at $T^+ = 4$, which leads to the appearance of an intersection point. The LJ vapor–liquid equilibrium density values at $T^+ = 0.8$ are about $\rho^+_{\text{vap,VLE}} = 0.006$ and $\rho^+_{\text{liq,VLE}} = 0.8$ [7], respectively, while the liquid density at solid–fluid equilibrium is about $\rho^+_{\text{liq,SFE}} = 0.88$ [8]. Eq. (6) (Table 1) hence acts, at $T^+ = 0.8$, as an interpolation tool in the range $\rho^+_{\text{vap,VLE}}$, $\rho^+_{\text{liq,VLE}}$ and as an extrapolation tool for $\rho^+ > \rho^+_{\text{liq,SFE}}$. Fulfillment of restriction (9) guarantees the absence of loops in the viscosity versus density curve, at all temperatures. The increase of viscosity with temperature at zero density is the result of Eq. (7) for η^+_0, which gives a monotonically increasing η^+_0 as a function of T^+ throughout its full applicability range. At $T^+ = 0.5$ the LJ fluid is actually below its triple point temperature [8]. Therefore, it exists either as a low-density gas or as a high-density solid—it cannot exist as a dense fluid. Consequently the $T^+ = 0.5$ curve in Fig. 1 is thus, for most of its density range, the result of extrapolating fluid-state information available at higher temperature. Notice that the $T^+ = 0.5$ isotherm in Fig. 1 relates to the $T^+ = 0.8$ isotherm in a way qualitatively analogous to that of the $T^+ = 0.8$ isotherm with the $T^+ = 4$ isotherm. The $T^+ = 10$ (supercritical) curve in Fig. 1 also shows a proper qualitative behavior. If instead of Eq. (7), we had used at $T^+ = 10$ the equation available in Ref. [5] for η^+_0, then, the low-density part of the $T^+ = 10$ isotherm would have fallen below the $T^+ = 0.8$ isotherm, which would not have been acceptable.

Fig. 2 shows a set of viscosity versus temperature isochors generated using Eq. (6) (Table 1), in the T^+ range from 0.3 to 10. The two vertical dashed lines indicate the extreme values of T^+ of the RP [5] LJ simulation data. Outside such temperature range, Fig. 2 shows values of viscosity, which are extrapolations, except for the zero density isochor, which Eq. (7) fully sets. It can be seen that Eq. (6) (Table 1) produce smooth and well-behaved extrapolations of the supporting molecular simulation data. The thick solid vertical line corresponds to the LJ critical value of T^+ [9], while the thin vertical solid line identified as TP corresponds to the LJ triple point value of T^+ ([8]). At high-density viscosity decreases with temperature, i.e., the behavior is the opposite to that shown at low density. At intermediate densities the isochors show minima. This rich behavior comes from the fact that, while the first term of the right hand side of Eq. (6) is a monotonically increasing function of T^+, the second double summation term, used with positive b_{ij} parameters [restrictions (15)], is a monotonically decreasing function of T^+. Notice that both terms in Eq. (6) used with Table 1 parameters are always positive. The appearance of Fig. 2 would not have changed had we generated it for much wider ranges of T^+ and ρ^+. This is true as long as the (very wide) T^+ range of Eq. (7) is not violated. This is a very important feature of the present model.

Eq. (6) (Table 1) makes it possible on one hand to avoid performing a long molecular simulation run every time that a viscosity value for the Lennard–Jones fluid is required. On the other hand it acts as an smoothing equation on the raw RP [5]

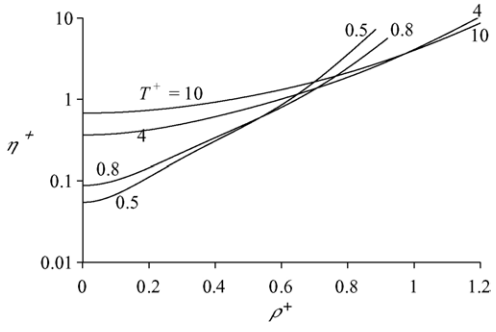

Fig. 1. Viscosity vs. density isotherms for the Lennard–Jones fluid generated using Eq. (6) (Table 1).

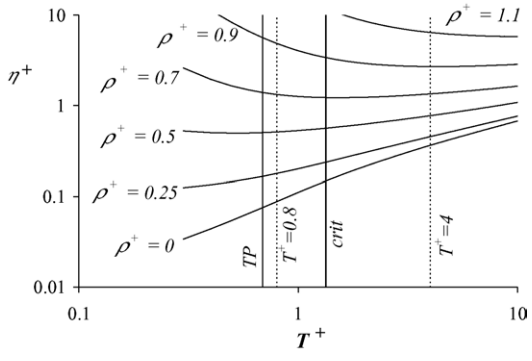

Fig. 2. Lennard–Jones (LJ) reduced viscosity as a function of the LJ reduced temperature at varying density values. The dashed vertical lines enclose the temperature range of the supporting RP [5] molecular simulation data. The solid vertical lines indicate the range from the LJ triple point temperature [8] to the LJ critical point temperature [9].

molecular simulation data. Finally, outside the temperature range of the RP data (both at high and low temperatures), Eq. (6) (Table 1), which depends on the zero-density viscosity values which Eq. (7) provides, generates acceptable extrapolations of the RP data. Notice that Eq. (6) (Table 1) is applicable to the Lennard–Jones fluid at any fluid state: gas, liquid or supercritical fluid. However, later in this work, we limit the real-fluid LJ-based modeling of viscosity to supercritical conditions only.

5. Lennard–Jones PVT analytical representation

The usual engineering need is to calculate viscosities at a given temperature and pressure rather than at given temperature and density. Kolafa and Nezbeda [9] proposed an analytical EOS for the Lennard–Jones fluid, i.e., the PVE/hBH LJ-EOS, which interrelates the temperature, the pressure, and the density of the LJ fluid. The PVE/hBH LJ-EOS is based on critically assessed computer simulation data from several sources. We use such equation here in combination with Eq. (6) to calculate viscosities at given temperature and pressure. The PVE/hBH LJ-EOS is the following:

$$z = \frac{P^+}{\rho^+ T^+} = f_{\mathrm{KN}}(\rho^+, T^+) \tag{16}$$

where z is the compressibility factor and f_{KN} is a function of $\rho^+$and T^+ available in the original Ref. [9] and more concisely in Ref. [4]. The temperature range of applicability of Eq. (16) is $0.68 \leq T^+ \leq 10$. The range for ρ^+ is from 0 (zero) to the density of the dense LJ fluid in equilibrium with the LJ solid ($\rho^+_{\mathrm{fluid,SFE}}$). Here, we mean by solid–fluid equilibrium situations not corresponding to the equilibrium between the solid and a low-density vapor which for the LJ fluid happens at T^+ less than about 0.68. Kolafa and Nezbeda [9] built Eq. (16) without imposing constraints related to the location of the critical point. Hence, the PVE/hBH EOS is a classical Lennard–Jones EOS. This is not problematic due to small critical enhancement for viscosity. The critical coordinates corresponding to Eq. (16) are the following [9]:

$$T_c^+ = 1.3396 \tag{17}$$

$$P_c^+ = 0.1405 \tag{18}$$

$$\rho_c^+ = 0.3108 \tag{19}$$

The value of T_c^+ implies that the RP [5] LJ viscosity data correspond to a maximum temperature of roughly 3 times the critical temperature. Zabaloy et al. [4] presented a procedure to compute $\rho^+_{\mathrm{fluid,SFE}}$. In this work, which is ultimately limited to temperatures such that $T^+ \geq T_c^+$, the computed ρ^+ values were always less than $\rho^+_{\mathrm{fluid,SFE}}$. On the other hand, the T^+ range of Eq. (16) was never exceeded.

It can be shown that Eq. (16) generates pressure versus density isotherms at subcritical temperatures, which contain pressure ranges where there are two meaningful values of density (vapor and liquid) at a given (positive) pressure.

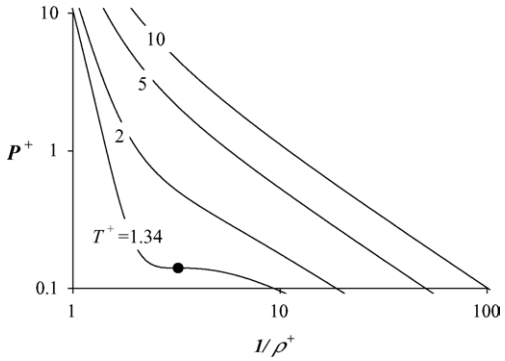

Fig. 3. Pressure as a function of reduced molar volume for the Lennard–Jones fluid at supercritical temperatures and mostly at supercritical pressures. We generated the curves using Eq. (16). (●) Critical point.

Fig. 3 shows the pressure P^+ as a function of the inverse density for four isotherms corresponding to temperature values greater than or equal to the critical temperature. All curves correspond to Eq. (16). Most of the pressure range in Fig. 3 is supercritical. The variable $1/\rho^+$ is a reduced molar volume. The critical isotherm shows a characteristic flat region where the volume is very sensitive to small changes in pressure. Fig. 3 indicates that at a given supercritical T^+ value there is only one ρ^+ value compatible with a given P^+ value.

6. Combining LJ viscosity and PVT analytical representations

Fig. 4 shows the Lennard–Jones reduced viscosity η^+ as a function of the practical reduced temperature T_r ($=T/T_c$) at varying values of the practical reduced pressure P_r ($=P/P_c$). Here, T_c and P_c are, respectively, the critical temperature and critical pressure. We generated Fig. 4 by combining basically Eqs. (16) and (6) (Table 1). We provide more details in Appendix A. The curve labeled "$P_r = 0$" corresponds to zero density. Hence, it is a direct result of Eq. (7). The curve labeled "$P_r = 0$ (liq)" corresponds to liquid viscosities at the limit of zero pressure. This curve exists because Eq. (16) provides liquid-like roots at zero pressure at low enough temperatures. The "$P_r = 1$" curve is the critical isobar which shows a steep portion typical of the critical region and a minimum characteristic of the transition from lower to higher temperatures. Minima appear also at higher pressures. The behavior, which Fig. 4 depicts is in essential agreement with that found in real fluids. Zabaloy et al. [4] generated a similar figure, which was however limited to the temperature range indicated with vertical dashed lines in Fig. 4. Such temperature range is the range of the RP supporting molecular simulation data [5]. The full temperature range of Fig. 4 curves is basically the same than the applicability range of Eq. (16) which is much wider (max T_r is about 7.5) than that of the RP viscosity data

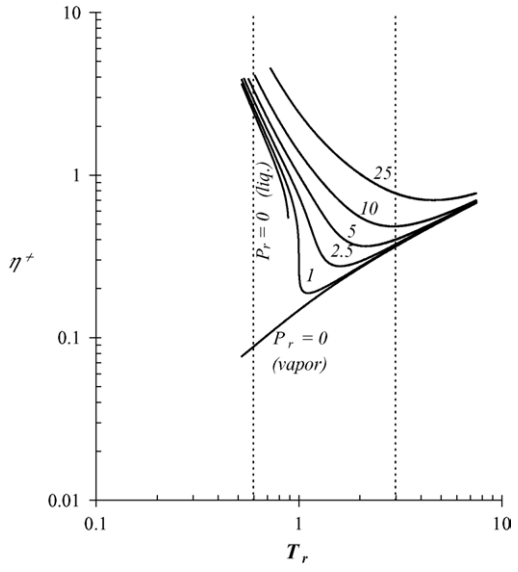

Fig. 4. LJ reduced viscosity η^+ as a function of the practical reduced temperature T_r (=T/T_c) for the Lennard–Jones Fluid at varying practical reduced pressure P_r(=P/P_c) values. The vertical dashed lines indicate the temperature range of the supporting RP LJ molecular simulation data [5] (see Appendix A for details).

[5]. At T_r higher than about 3 in Fig. 4; Eq. (6) (Table 1) actually acts, on the supporting molecular simulation data, as an extrapolation equation and it gives a proper shape for the isobars at such higher temperatures. Notice that the rich variety of trends for the viscosity as a function of temperature and pressure depicted in Fig. 4 is basically implied by the simple intermolecular potential function defined by Eq. (1), i.e., no experimental real fluid viscosity data were used at all for generating Fig. 4.

For known values of m, ε and σ the viscosity η at given temperature T and pressure P is calculated as follows: (a) calculate T^+ [Eq. (2)] and P^+ [Eq. (3)]; (b) calculate ρ^+ using Eq. (16); (c) calculate η^+ using Eq. (6); (d) calculate η from Eq. (5).

Viscosity diverges at the critical point (see, e.g., Ref. [17]). Yet, Eq. (6) does not account for the critical enhancement for viscosity that takes place in the neighborhood of the critical point. In contrast with the case of the thermal conductivity, the critical enhancement in viscosity is small and becomes important only within a narrow region around the critical point [4]. Therefore, the present model does not account for such critical enhancement effect. This is not noticeably important, in view of the fact that supercritical extraction and processing is carried out at conditions far enough from the region where the solvent critical enhancement effect takes place (see Ref. [4] for more details). Eqs. (6) and (16), which apply to the LJ fluid, interrelate sets of dimensionless variables. The LJ fluid is therefore a corresponding states fluid where the dimensionless variables have, as a distinguishing feature, a dependency on parameters meaningful at molecular level.

7. Real-fluid LJ-based viscosity modeling: compound-specific parameters

To explore the potential of a LJ-based modeling of the viscosity of pure fluids, Zabaloy et al. [4] assumed that a real fluid behaves as a LJ fluid having a critical temperature T_c and a critical pressure P_c exactly matching the real fluid experimental values. Such assumption is equivalent to supposing that real fluids behave as LJ fluids with effective intermolecular potential parameters consistent with the experimental critical coordinates. The viscosity predictions were [4] thus based only on molecular weight, T_c and P_c [4]. For a given pure compound the parameters ε and σ are forced to match the experimental values of T_c and P_c by combining Eqs. (2), (3), (17) and (18) with the experimental values of T_c and P_c. For reasons that will become clear below, we define σ_c as the value of σ computed, as described, from the experimental T_c and P_c (see Appendix B for details).

The LJ-based model of Ref. [4] has an unknown qualitative behavior beyond the density and temperature ranges of the supporting molecular simulation data. Besides, it is purely predictive, i.e., the viscosity of a given pure fluid at set temperature and pressure is computed from the molecular weight and from the experimental values of T_c and P_c. Such a limited input information is not enough to quantitatively represent the viscosity of real fluids whose molecules are polar and/or non-spherical. Ruckenstein and Liu [10] studied the LJ-based modeling of self-diffusion coefficients. They found such property to be more sensitive to σ than to ε. Following Ruckenstein and Liu [10], we here set σ, in a way, as an adjustable parameter set to match experimental viscosities. A constant value for σ, different from σ_c, giving, in certain temperature–density region, better numerical values of viscosity than σ_c, would imply a critical pressure different from the experimental one. To solve this dilemma we decided to set σ as temperature dependent. The use of temperature dependent LJ parameters is valid for engineering purposes [11]. In this work we set σ as a linear function of the practical reduced temperature, as follows:

$$\alpha_\sigma = \frac{\sigma}{\sigma_c} = 1 + S_\sigma(T_r - 1) \tag{20}$$

From Eq. (20), it is evident that at the critical temperature σ becomes equal to its critical value σ_c and hence consistency with the experimental critical T, P coordinates is kept. In this work, we set the (dimensionless) slope s_σ as an adjustable parameter, which we fit against experimental viscosities. On the other hand, we kept ε constant, i.e., equal to its critical value, at all temperatures. From Eq. (20) it is clear that, unless we introduce another adjustable parameter, the viscosity along the critical isotherm, where $T_r = 1$, becomes completely set by the experimental values of T_c and P_c and by the molecular weight. To gain a degree of freedom to remove such limitation we introduce now a second

adjustable parameter defined as follows:

$$\eta = \frac{F\eta^{+}\sqrt{m\varepsilon}}{\sigma^2} \tag{21}$$

Notice that at $F = 1$ Eqs. (5) and (21) become identical. F is a dimensionless corrective parameter, which acts directly on the LJ viscosity (which is equal to $\eta^{+}\sqrt{m\varepsilon}/\sigma^2$). From the practical point of view, parameter F has on the LJ viscosity a role analogous to parameter A_D on the LJ self diffusion coefficient in Ref. [10]. The parameter A_D [10] is the translational–rotational coupling factor, which accounts for the non-spherical nature of real fluid molecules. To illustrate the use of the above equations we provide a calculation example in Appendix B.

8. Results and discussion

Table 2 shows results for the Lennard–Jones based modeling of the viscosity of supercritical pure fluids. Table 2 also shows, for every pure compound, details about the database we used in this work, i.e., the temperature and pressure ranges and the number of experimental data points. The total number of experimental data points is 2844. The two "Prediction Results" columns show the average and maximum percent deviations when no adjustable parameters are used, i.e., for $F = 1$ and $s_\sigma = 0$. In such a case, the only input experimental information used was the critical temperature, critical pressure and the molecular weight, which we took from Ref. [12]. From the AAD% values in Table 2, we can conclude that compounds such as propane, carbon dioxide, nitrogen and *n*-butane can be treated, within the temperature and pressure ranges of Table 2, as LJ fluids having constant effective ε and σ parameters set to reproduce the pure compound experimental critical temperature and critical pressure. For fluids, such as water or hydrogen sulfide, such an approach is not acceptable from the quantitative point of view.

Table 2 also shows correlation results in the last four columns. For every given compound, we adjusted simultaneously the F and s_σ parameters. Parameter F is normally close to unity.

The values for the slope s_σ corresponded always to values of α_σ in the order of unity (roughly in the range 0.8–1.2). It can be seen that the average deviation for all compounds except water is now less than or equal to 7%, which is within the experimental uncertainty for viscosity at high pressure. Thus, Eq. (20) makes possible to considerably reduce the model errors keeping a narrow enough range of variation for variable α_σ while preserving consistency with the pure compound critical pressure.

The only regularity that Table 2 shows for the F parameter of the *n*-alkanes is that its value is of the order of unity for all seven compounds. With regard to the *n*-alkane s_σ parameter, we observe in Table 2 a non-regular variation. These facts may be related to our parameter fitting procedure. We fitted every pair of parameters independently for every pure

Table 2
Prediction and correlation results for the Lennard–Jones based modeling of the viscosity of supercritical pure fluids

Compound	Reference	Number of experimental data points	Min T_r	Max T_r	Min P_r	Max P_r	Prediction results		Correlation results			
							AAD% at $F = 1$ and $S_\sigma = 0$	Max AD% at $F = 1$ and $S_\sigma = 0$	F (no units)	s_σ (no units)	AAD%	Max AD%
Methane	[13]	176	1.68	2.73	1.00	15.2	11	15	1.0356	−0.0443	2	6
Ethane	[13]	170	1.05	2.29	1.00	14.4	7	12	1.0516	−0.0390	3	8
Propane	[13]	168	1.08	2.03	1.00	8.2	4	10	1.0351	−0.0102	2	7
n-Butane	[13]	191	1.06	1.88	1.00	18.4	6	28	0.9321	−0.1109	7	17
n-Pentane	[13]	160	1.04	1.81	1.00	14.8	9	18	1.0815	−0.0192	3	11
n-Heptane	[13]	112	1.02	1.15	1.00	18.2	10	24	1.1047	0.0929	6	13
n-Octane	[13]	25	1.1	1.18	1.00	20.1	10	19	1.0680	−0.0834	6	14
iso-Butane	[13]	254	1.03	2.08	1.00	13.7	7	24	1.0056	−0.0086	6	23
iso-Pentane	[13]	143	1.02	1.63	1.18	17.8	15	28	1.1785	−0.0317	4	15
2-2-Dimethylpropane (neopentane)	[14]	9	1.02	1.02	1.29	17.3	29	33	1.4040	−1.3638	1	4
Ethylene	[13]	285	1.06	2.48	1.00	15.9	7	15	1.0600	−0.0316	4	10
Propylene	[13]	357	1.04	1.78	1.00	19.6	11	39	1.1204	0.0143	4	31
Carbon dioxide	[13]	347	1.02	2.96	1.00	13.5	5	15	1.0285	−0.0085	4	13
Water	[15]	184	1.01	1.50	1.04	3.6	18	33	1.0349	−0.4467	11	22
Nitrogen	[13]	230	2.14	3.57	1.18	29.4	5	9	1.0000	−0.0243	2	5
Hydrogen sulfide	[16]	33	1.04	1.11	1.12	5.6	45	72	1.8110	1.1616	6	27

compound, giving the same weight to every experimental data point during the optimization course. For a given pure compound, a finer procedure would consist of splitting the temperature–pressure plane into constant area sub-regions and ascribe the same weight factor to every sub-domain regardless of the number of data points falling within each of them. This procedure would result in a more balanced performance of the model and would lead to values for F and s_σ surely different from those we reported in Table 2, which might follow more regular variations for the n-alkanes.

Despite the non-regular s_σ variation for the n-alkane homologous series, it can be shown, for any given n-alkane listed in Table 2, that the maximum departure of parameter σ from the σ average value falls in the range from 1 to 5%, within the temperature range reported in Table 2 for the chosen n-alkane. Such variability is much less than that of the original viscosity data. On the other hand, as Fig. 5 shows, the average value of σ is a monotonically increasing function of molecular weight for n-alkanes at the temperature ranges and (non-zero) s_σ values which Table 2 reports. Hence, the average value of σ roughly follows a regular variation for n-alkanes. Notice that σ rather than s_σ is the parameter to be averaged when modeling mixtures.

For the n-alkanes (or any other homologous series) it would be possible to set, e.g., linear variations with respect to molecular weight for both, parameter F and parameter s_σ. Such approach would provide four parameters to be fit against all the n-alkane data simultaneously, in comparison to the two parameters per n-alkane we used here. The homologous-series-specific four parameter approach would provide, by construction, regular variations for parameters F and s_σ of the n-alkane family of compounds, with an expected overall quantitative model performance intermediate between the two we show in the last six columns of Table 2.

As it is evident from Eq. (1), the Lennard–Jones fluid is made of spherical molecules, while none of the fluids listed in Table 2 does. On top of that, fluids, such as water and hydrogen sulfide have a polar nature, which seems to explain the relatively large value for, e.g., parameter s_σ, for both compounds. In our opinion, the Lennard–Jones fluid is anyway a good reference fluid not only because it qualitatively behaves as real fluids do, but also because of the availability in the literature of molecular simulation data (transport and thermodynamic properties) at a large number of conditions. The present model accounts for the non-Lennard–Jones nature of real fluids through parameters F and S_σ an trough the experimental values of the T_c and P_c.

When $F \neq 1$ and/or $S_\sigma \neq 0$, the present model transforms, for a chosen pure compound, the experimental viscosity data, together with the experimental critical temperature and critical pressure, into (always positive) values of F, ε and σ, which could be used to represent the viscosity of mixtures of supercritical fluids through proper mixing rules. Parameters F and ε are both constant, while the temperature-dependent σ parameter has a variability less than that of viscosity itself. Basically, the present model makes possible to encapsulate the observed experimental behavior for viscosity, within a Lennard–Jones formalism as a step for modeling mixtures. Because of this, the values we report in Table 2 for parameters F and s_σ should not be regarded as the result of just a fitting exercise. In other words, if for a given pure compound listed in Table 2, we simply correlated the viscosity as an, e.g., explicit polynomial function of temperature and pressure, we would require a number of compound-specific fitting parameters larger than two, to achieve a performance equivalent to that in the last two columns of Table 2. Such parameter values most likely would have varying signs and magnitudes and hence it would not be possible to define proper mixing rules for them when modeling mixtures.

From the previous paragraph it is clear that for modeling mixtures the present approach would require mixing rules for parameters F and ε; for parameter σ, but not for the slope s_σ.

For supercritical nitrogen the T^+ range of the RP LJ data [5] was exceeded reaching T^+ a maximum value of about 4.8 (see Appendix B).

Figs. 6–9 show correlation results for four supercritical pure compounds. In all cases, the markers correspond to experimental data, while the lines are the model correlation results, corresponding to the last four columns of

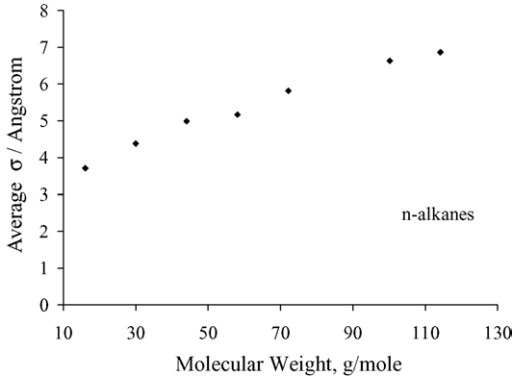

Fig. 5. Average value of the temperature-dependent σ parameter as a function of molecular weight for normal alkanes from methane to n-octane. For a given n-alkane, the average σ value corresponds to the non-zero S_σ value and to the temperature range, which Table 2 reports.

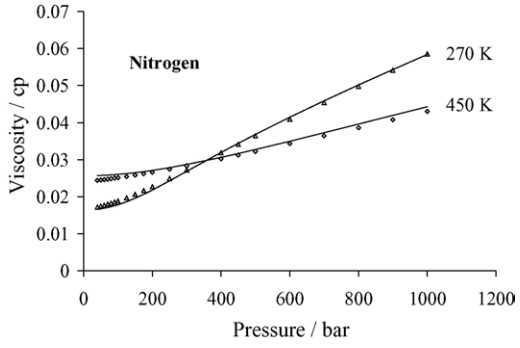

Fig. 6. Correlation (curves) of viscosity data ((△), (◊), [13]) for supercritical nitrogen.

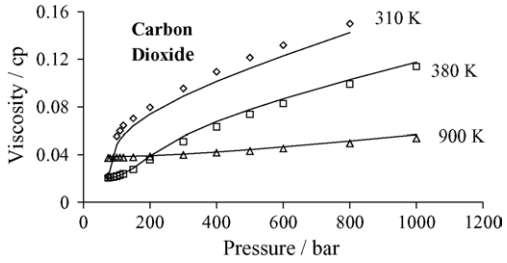

Fig. 7. Correlation (curves) of viscosity data ((◊), (□), (△), [13]) for supercritical carbon dioxide.

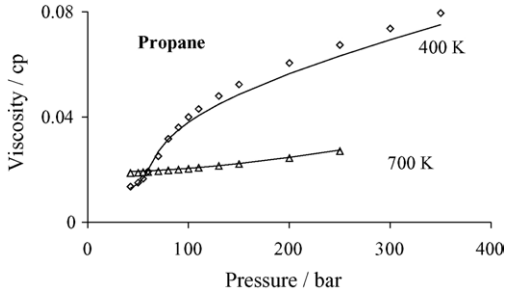

Fig. 8. Correlation (curves) of viscosity data ((◊), (△), [13]) for supercritical propane.

Table 2. Fig. 6 shows the viscosity as a function of pressure for supercritical Nitrogen at two temperatures. The highest temperature (450 K) corresponds to a T^+ value beyond the maximum value of the LJ viscosity data we used to build Eq. (6) (Table 1). Evidently the extrapolation schemes embedded within Eq. (6) (Table 1) worked well for Nitrogen, e.g., the model correctly describes the occurrence of an intersection point and properly follows the experimental data.

Figs. 7 and 8 show the model viscosity and the experimental viscosity as a function of pressure for supercritical CO_2 and supercritical propane, respectively, at different temperatures. Fig. 9 shows correlation results (in this case viscosity as a function of temperature for different isobars) for supercritical *n*-heptane. For all of these cases, the pressure range is wide. It can be seen that the model reproduces with a good level of accuracy the observed viscosities both, at qualitative and quantitative level. Notice that the present model is able to condense within the values of the parameters F and s_σ the relatively complex topology of the supercritical viscosity-pressure-temperature surface, of which Figs. 6–9 are examples. In other words, the present model represents the viscosity surface of a given pure component as a point in the (S_σ, F) plane.

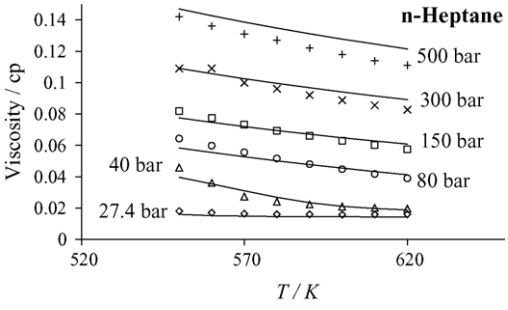

Fig. 9. Correlation (curves) of viscosity data ((+), (×), (□), (◯), (△), (◊), [13]) for supercritical *n*-heptane.

9. Remarks and conclusions

In this work, we provide an analytical equation (Eq. (6)) for the relationship among viscosity, temperature and density for the Lennard–Jones fluid. Such analytical equation has a better performance than another one developed previously [4]. Eq. (6) matches a zero-density Chapman–Enskog LJ viscosity expression (Eq. (7)), which has an extremely wide temperature range of applicability. The LJ VTD relationship, i.e., Eq. (6), has a functional form which, for positive values of its parameters (Table 1), guarantees a proper qualitative behavior for the viscosity at any density and at any temperature within the wide temperature range of Eq. (7). Thus, Eq. (6) coupled to the parameters in Table 1 properly extrapolates the LJ molecular simulation data on which it is based. The trends for the viscosity as a function of density and temperature available to Eq. (6) are less varied than those found for real fluids. This is acceptable, since we use here Eq. (6) as a basis for a general model designed to work over a wide range of conditions.

The equations we presented here clearly show the corresponding states nature of the Lennard–Jones fluid. The hallmark of a LJ based corresponding states approach is that its dimensionless variables are defined in terms of parameters meaningful at molecular level.

The advantage of corresponding states (CS) approaches is that once the user makes sure that the model qualitative trends are acceptable in the space of the reduced variables, the qualitative trends will, in general, also be acceptable for any real fluid represented by such CS model.

However, strictly, from the quantitative point of view, real fluids are neither “corresponding fluids” nor do they have a Lennard–Jones nature. On one hand, we partially overcome this limitation by representing a given real fluid as a LJ fluid having a critical temperature and a critical pressure identical, respectively, to the real fluid experimental critical temperature and experimental critical pressure. When such predictive reference is not enough to achieve a good quantitative performance, we introduce two parameters (S_σ, F), which we fit against viscosity experimental information. The parameters (S_σ, F) are compound-specific and do not affect Eq. (6), which has parameters (Table 1) which are not compound-specific. In this way, we have shown here that it is possible to represent with a good level of accuracy the viscosity of pure real supercritical fluids over a wide range of conditions, in terms of effective parameters with some meaning at molecular level. The present approach requires the knowledge of the molecular weight, the experimental critical temperature and the experimental critical pressure.

The good qualitative behavior of Eq. (6) is convenient for an adequate model performance not only when calculating viscosity values but also when adjusting the parameters F and s_σ for a chosen pure real fluid.

Another distinguishing feature of the present approach is that the user computes the required density values from a LJ equation of state, i.e., from Eq. (16). Therefore, the present approach uses a LJ reference not only for the viscosity–temperature–density relationship (Eq. (6)) but also for the pressure–temperature–density relationship (Eq. (16)). In this regard, the model presented here is somewhat more consistent than other approaches. In other words, the user does not have to resort to compound-specific correlations for calculating the density, which in this work plays the role of an intermediate variable. The model correlates the pure compound viscosity of real supercritical fluids over a wide range of conditions with average absolute-value relative deviations less than or equal to 7 % (excluding water).

Acknowledgements

The authors are grateful to Professor Erling H. Stenby and Mr. Claus Zéberg-Mikkelsen (Technical University of Denmark) for having provided a viscosity database; to Miss Eliana Abreu for helping to prepare the final digital version of the viscosity database used here; for financial support, to the European Commission (EVIDENT project, Contract No: JOF3-CT97-0034), to Consejo Nacional de Investigaciones Científicas y Técnicas de la República Argentina, and to University of Nevada, Reno.

Appendix A. Generation of Fig. 4

From Eqs. (2) and (3) it can be, respectively, shown that, if the LJ parameters ε and σ are regarded as constant, then

$$T^+ = T_r T_c^+ \tag{A.1}$$

$$P^+ = P_r P_c^+ \tag{A.2}$$

We generated Fig. 4 applying the following calculation procedure:

- Set the value or T_r and calculate T^+ using Eq. (17) of the text and Eq. (A.1).
- Compute η_0^+ from Eq. (7) of the text.
- Set the value of P_r and calculate P^+ using Eq. (18) of the text and Eq. (A.2).
- From the computed values of T^+ and P^+ calculate the density ρ^+ using Eq. (16) of the text.
- Compute η^+ from Eq. (6) (with parameters from Table 1).

The fourth step can give up to three values of ρ^+ being the middle one meaningless. The two meaningful values, when they exist, lead to two values of viscosity (a liquid-like one and a vapor-like one)

When generating Fig. 4 we never exceeded the density of the dense LJ fluid at solid–fluid equilibrium, i.e., $\rho^+_{\text{fluid,SFE}}$.

Appendix B. Sample viscosity calculation for supercritical nitrogen

The first step consists of computing the parameters ε and σ_c. For that, we first combine Eqs. (2), (3), (17) and (18) to give

$$T_c^+ = 1.3396 = \frac{\kappa T_c}{\varepsilon} \tag{B.1}$$

$$P_c^+ = 0.1405 = \frac{P_c \sigma_c^3}{\varepsilon} \tag{B.2}$$

Notice that we have added the subscript "c" to σ because in the present model we made σ temperature dependent.

In the present model, we force the reproduction of the experimental pure compound critical temperature T_c and pressure P_c by introducing such experimental information into Eqs. (B.1) and (B.2), which we then solve for ε and σ_c, being the result:

$$\varepsilon = \frac{\kappa T_c}{T_c^+} = \frac{\kappa T_c}{1.3396} \tag{B.3}$$

$$\sigma_c = \left(\frac{\kappa T_c}{P_c}\frac{P_c^+}{T_c^+}\right)^{1/3} = \left(\frac{\kappa T_c}{P_c}\frac{0.1405}{1.3396}\right)^{1/3} \tag{B.4}$$

Eq. (16) of the text gives an exact reproduction of the experimental values of T_c and P_c if the user computes ε and σ_c from Eqs. (B.3) and (B.4). Table B.1 illustrates the use of the present model. The sample problem statement is the following: Calculate the viscosity of Nitrogen at 450 K and 1000 bar. As shown in Table B.1, the result is in this case $\eta = 442.8$ μP. In this example, Eq. (16) has only one density root. This is always the case if $T^+ \geq T_c^+$. Notice that in this example T^+ exceeds the range of the supporting molecular simulation data (Ref. [5], $0.8 \leq T^+ \leq 4$) and hence Eq. (6) (Table 1) acts as an extrapolation prescription. Also observe

Table B.1
Sample viscosity calculation

Input data		Calculated variables	
Compound	Nitrogen	ε/k (K), Eq. (B.3)	94.21
M_w (g mol^{-1}) [12]	28.0135	σ_c (Å), Eq. (B.4)	3.774
T_c (K) [12]	126.2	P_r (=P/P_c)	29.41
P_c (bar) [12]	34	T_r (=T/T_c)	3.57
s_σ (Table 2)	−0.0243	α_σ, Eq. (20)	0.9377
F (Table 2)	1.0000	σ (Å), Eq. (20)	3.539
T (K)	450	T^+, Eq. (2)	4.7767036
P (bar)	1000	$\rho^+_{\text{fluid},SFE}$ Ref. [4]	1.288
		η_0^+, Eq. (7)	0.4127344
		η_0 (μP), Eq. (21)	256.4
		P^+, Eq. (3)	3.4074754
		ρ^+, Eq. (16)	0.4369971
		η^+, Eq. (6) (Table 1)	0.7129746
		η (μP), Eq. (21)	442.8

that we did not need to calculate the (dimensionful) value of ρ in order to quantify the viscosity. Rather, it sufficed to compute the value of ρ^+, which, as we show in Table B.1, is roughly equal to one third of the maximum fluid density ($\rho^+_{\text{fluid,SFE}}$) at which Eq. (16) is applicable.

References

[1] J.F. Ely, H.J.M. Hanley, Prediction of transport properties. 1. Viscosity of fluids and mixtures, Ind. Eng. Chem. Fundam. 20 (1981) 323.

[2] K.E. Gubbins, Application of molecular theory to phase equilibrium predictions, in: S.I. Sandler (Ed.), Models for Thermodynamic and Phase Equilibria Calculations, Marcel Dekker, Inc., New York, 1994, p. 508.

[3] T.F. Sun, J. Bleazard, A.S. Teja, A method for the prediction of the transport properties of dense fluids: application to liquid *n*-alkanes, J. Phys. Chem. 98 (1994) 1306.

[4] M.S. Zabaloy, J.M.V. Machado, E.A. Macedo, A study of Lennard–Jones equivalent analytical relationships for modeling viscosities, Int. J. Thermophys. 22 (2001) 829.

[5] R.L. Rowley, M.M. Painter, Diffusion and viscosity equations of state for a Lennard–Jones fluid obtained from molecular dynamics simulations, Int. J. Thermophys. 18 (1997) 1109.

[6] R.C. Reid, J.M. Prausnitz, B.E. Poling, The Properties of Gases & Liquids, fourth ed., McGraw-Hill International Edition, New York, 1987, pp. 392–393.

[7] M. Mecke, A. Müller, J. Winkelmann, J. Vrabec, J. Fischer, R. Span, W. Wagner, An accurate van der waals-type equation of state for the Lennard–Jones fluid, Int. J. Thermophys. 17 (1996) 391 (also Erratum 1 in Int. J. Thermophys., 19 (1998) 1493).

[8] R. Agrawal, D.A. Kofke, Thermodynamic and structural properties of model systems at solid–fluid coexistence. II. Melting and sublimation of the Lennard–Jones system, Mol. Phys. 85 (1995) 43.

[9] J. Kolafa, I. Nezbeda, The Lennard–Jones fluid: an accurate analytic and theoretically-based equation of state, Fluid Phase Equilib. 100 (1994) 1.

[10] E. Ruckenstein, H. Liu, Self-diffusion in gases and liquids, Ind. Eng. Chem. Res. 36 (1997) 3927.

[11] T. Sun, A.S. Teja, Vapor–liquid and solid–fluid equilibrium calculations using a Lennard–Jones equation of state, Ind. Eng. Chem. Res. 37 (1998) 3151.

[12] DIPPR 801, Evaluated Process Design Data, Public Release, American Institute of Chemical Engineers, Design Institute for Physical Property Data, BYU-DIPPR, Thermophysical Properties Laboratory. Provo, Utah, 1998.

[13] K. Stephan, K. Lucas, Viscosity of Dense Fluids, Plenum Press, New York/London, 1979.

[14] H. Gonzalez, A.L. Lee, Viscosity of 2,2-dimethylpropane, J. Chem. Eng. Data 13 (1968) 66.

[15] N.B. Vargaftik, Tables on the Termophysical Properties of Liquids and Gases, second ed., Hemisphere Publishing Corporation, Washington/London, 1975.

[16] J.M. Monteil, F. Lazarre, J. Salvinien, P. Viallet, Viscosimétre a mesures relatives pour étude de H2S gazeux au voisinage du point critique, J. de Chim. Phys. 66 (1969) 1673.

[17] J.T.R. Watson, R.S. Basu, J.V. Sengers, An improved representative equation for the dynamic viscosity of water substance, J. Phys. Chem. Ref. Data 9 (1980) 1255.